

INDUCTION STUDIES WITH SATELLITE DATA

NILS OLSEN

Danish Space Research Institute, Juliane Maries Vej 30, 2100 Copenhagen Ø, Denmark

Abstract. The natural variations of the Earth's magnetic field of periods spanning from milliseconds to decades can be used to infer the conductivity-depth profile of the Earth's interior. Satellites provide a good spatial coverage of magnetic measurements, and forthcoming missions will probably allow for observations lasting several years, which helps to reduce the statistical error of the estimated response functions.

Two methods are used to study the electrical conductivity of the Earth's mantle in the period range from hours to months. In the first, known as the potential method, a spherical harmonic analysis of the geomagnetic field is performed, and the Q -response, which is the transfer function between the internal (induced) and the external (inducing) expansion coefficients is determined for a specific frequency. In the second approach, known as the geomagnetic depth sounding method, the C -response, which is the transfer function between the magnetic vertical component and the horizontal derivative of the horizontal components, is determined. If one of these transfer functions is known for several frequencies, models of the electrical conductivity in the Earth's interior can be constructed.

This paper reviews and discusses the possibilities for induction studies using high-precision magnetic measurements from low-altitude satellites. The different methods and various transfer functions are presented, with special emphasis on the differences in analysing data from ground stations and from satellites. The results of several induction studies with scalar satellite data (from the POGO satellites) and with vector data (from the Magsat mission) demonstrate the ability to probe the Earth's conductivity from space. However, compared to the results obtained with ground data the satellite results are much noisier, which presumably is due to the shorter time series of the satellite studies.

The results of a new analysis of data from the Magsat satellite indicate higher resistivity in oceanic areas than in continental areas. However, since this holds for the whole range of periods between 2 and 20 days, this difference probably is not caused purely by differences in mantle conductivity (for which one would expect less difference for the longer periods). Further studies with data from recently launched and future satellites are needed.

Keywords: electrical conductivity, geomagnetic induction, geomagnetic satellites, mantle

1. Introduction

Studying the Earth's conductivity with satellites is explicitly mentioned as a research topic for all high-precision geomagnetic missions. With this interest in induction studies from space in mind, it is surprising to find only very few publications on that topic, at least in comparison with other aspects of satellite studies. One reason for this is given by the fact that until now only one satellite acquired the high-precision data that are necessary for induction studies, namely Magsat in 1979/80. Despite its relatively short lifetime of only 7 months, the possibility of probing mantle conductivity from space has been demonstrated.



Surveys in Geophysics **20**: 309–340, 1999.

© 1999 Kluwer Academic Publishers. Printed in the Netherlands.

Although some missions were proposed as a continuation of Magsat, the scientific community has had to wait almost twenty years for the next high-precision geomagnetic mission. During the coming years, at least three satellites will measure the Earth's magnetic field from space, and additional missions are proposed. In comparison to Magsat they all carry improved instrumentation, have probably longer lifetimes, and offer the challenging possibility to perform joint analyses of simultaneous measurements from more than one satellite, all of which will certainly enhance the importance of induction studies from space.

Several successful attempts have been made to derive the (global) conductivity-depth distribution from magnetic satellite measurements. Contrary to this, the magnetic effect of conductivity anomalies on satellite data has only been investigated theoretically until now; it remains to be demonstrated that anomalies can be studied from space, as predicted by the model studies. Similarly, theoretical investigations exist of the question of how induction phenomena affect the estimation of other geomagnetic parameters, like crustal maps, but the results have not yet been verified by satellite observations.

The aim of this paper is to review and discuss the possibilities which magnetic measurements made from low-altitude satellites provide for induction studies.

Mantle conductivity can be studied in two ways: it can be probed "from below" using signals originating from the outer core. This method requires a precise determination of the field during rapid and isolated events (for instance geomagnetic "jerks"). It also requires some a priori assumptions about the kinematics of the fluid motion at the top of the core, since the core variations which reach the Earth's surface have been damped by the conductivity of the mantle. That is, the mantle behaves like a low-pass filter for the observed secular variation.

Mantle conductivity can also be studied "from the top" by the analysis of field changes of external origin, the induced currents of which modify the observed magnetic field variation.

Both methods require good knowledge of the time-space structure of the inducing field. The second approach is suitable for probing the conductivity down to depths of 1000 km or so, whereas the first approach has its strength in estimating the conductivity of the deep mantle. I will focus on the use of external (magnetospheric) variations for induction studies, but will also briefly mention satellite studies using internal signals (originating in the ionosphere or the core). Moreover, the paper concentrates on the study of the (global and large scale regional) mantle conductivity from space, since this is the topic for which the usefulness of satellite measurements has been demonstrated.

There are several advantages of using magnetic satellite data for induction studies:

- (i) Satellites sample the magnetic field over the entire Earth, which enables the estimation of true global responses which are not biased toward continental values (as it is the case for responses obtained from observatory data).

- (ii) The global coverage of the satellite data allows for studies of regional conductivity differences related, for example, to the distribution of oceans and continents.
- (iii) Measuring the magnetic field from an altitude of 400 km or so corresponds roughly to averaging over an area of this dimension. Thus the effect of local heterogeneities is reduced and hence regional response functions are less influenced by local conductivity anomalies.
- (iv) The data are obtained over different regions with the same instrumentation, which helps to reduce spurious effects when studying conductivity heterogeneities.

There are, however, some points to consider when using magnetic satellite data instead of ground based data for induction studies:

- (a) Since the satellite moves (with a velocity of about 8 km/s for an altitude of 400 km), it is not possible to decide whether an observed magnetic field variation is due to a temporal or spatial change.
- (b) It is necessary to measure the magnetic field with high accuracy – not only regarding resolution, but also regarding to orientation and absolute values. Only high-precision instrumentation allows to correct the data for core and crustal contributions, and thus prepare them for induction studies.
- (c) Due to the Earth's rotation, the satellite revisits a specific region after about one day.* Hence response functions for selected regions have to rely on time series with a sampling rate of 1 day. However, since the measurements were not low-pass filtered before "resampling", aliasing may occur.
- (d) Satellites measure the magnetic field at a few hundred kilometers altitude above ground. Depending on the method used, the estimated transfer functions may refer to the Earth's surface or to satellite heights (in which case they are not directly comparable to estimates obtained from ground based data). However, a transformation to ground values is straightforward if the space between ground and satellite is assumed to be free of primary and secondary sources, see Section 3.2.
- (e) Satellites usually acquire data not at one fixed altitude, but over a range of altitudes, which complicates the estimation of transfer functions. Depending on the method used, neglect of this height variation may add to the statistical error of the responses.
- (f) In order for the transfer functions to probe the Earth's conductivity, it is necessary that all currents below the observation point are entirely Earth induced. For induction studies with ground based data, this is mostly the case, but for satellite studies it may not be so. Ionospheric Sq currents, for instance, flow below the satellite orbit, and hence both the primary (inducing) currents in the ionosphere and the secondary (induced) currents in the Earth's interior are

* Actually the satellite revisits that region already after about 12 hours. but this will be for a different local time. For induction studies it is safer to rely on data taken at similar local time conditions, which results in the above stated sampling recurrence of 24 hours.

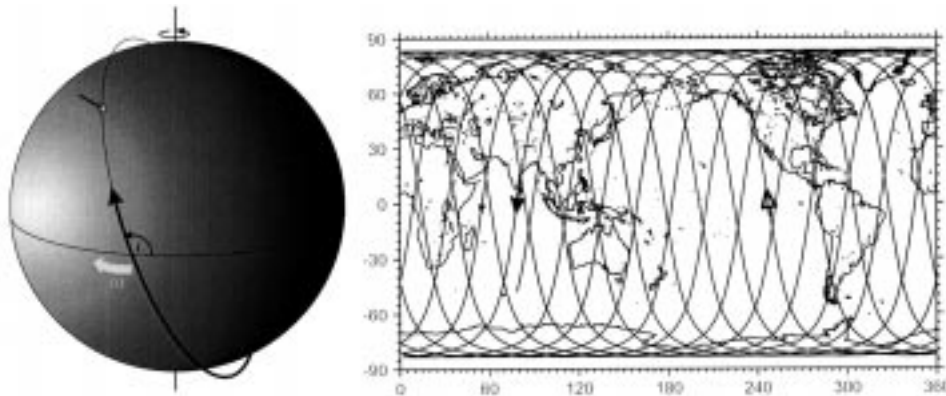


Figure 1. Left: The path of a satellite at inclination i in orbit around the rotating Earth. Right: Ground track of 24 hours of Magsat on January 1, 1980. The satellite starts at 0 UT at 68° N and 248° E, moves northward on the evening side of the Earth, crosses the polar cap, and continues southward on the morning side. It crosses the Equator at 79° E (large black arrow) during the dawn part of the orbit. After 45 minutes, the satellite crosses again the Equator, at 250° E (white arrow) while moving again northward. This is the dusk part of the orbit. The next Equator crossing (after additional 45 minutes) is at 55° E (small black arrow), 24° westward of the first crossing 90 minutes earlier.

of internal origin. However, induction studies with ionospheric currents are possible if satellite and ground data are combined, see Section 6.

- (g) Moreover, the region between the surface and the satellite has to be nonconducting. Even if there are no (primary) ionospheric currents and hence the previous item is fulfilled, a nonvanishing ionospheric conductivity would influence the response function because of secondary, induced, currents in the ionosphere. However, it will be shown in Section 3.3 that this distortion is much smaller than the present uncertainty and thus can safely be neglected.

The contents of the paper are as follows: Section 2 summarizes some properties of satellites for high-precision measurements of the Earth's magnetic field. Transfer functions for induction studies with satellite data are discussed in Section 3, and results of such studies are presented in Section 4. The effect of induction on magnetic satellite data on the basis of model studies is the topic of Section 5, and finally, in Section 6, some suggestions for future work are presented.

2. Measuring the Magnetic Field with Satellites

To understand magnetic measurements taken by satellites, some elementary facts about low-altitude satellites and their orbits might be helpful. The reader is referred to the first chapters of Langel and Hinze (1998) for an extended discussion and a list of references.

A satellite moves on an elliptical path with the center of mass of the Earth at one focus of the ellipse. The closest and farthest points from that point are perigee

TABLE I
High precision magnetic satellites

	Launch	Lifetime	Altitude	Local time
Magsat	Nov. 1979	7 months	250–550 km	6 ⁰⁰ /18 ⁰⁰
Ørsted	Feb. 1999	>14 month	600–850 km	all local times
SAC-C/Ørsted-2	Apr. 2000	>14 month	702 ± 5 km	10 ³⁰ /22 ³⁰
Champ	Apr. 2000	5 years	350–770 km	all local times

and apogee, respectively. The time for one full orbit varies with satellite height and is typically 90 minutes for a satellite at 400 km altitude. This gives roughly 15 orbits per day, and if the orbital plane is fixed with respect to space, the Earth's rotation will cause successive orbits to cross the equator at a longitude approximately $360^\circ/15 = 24^\circ$ more westward. An important parameter is the inclination i of the orbit (see the left part of Figure 1), which controls (together with apogee and perigee) the drift rate of the orbital plane. For $i = 90^\circ$, the orbital configuration is fixed in space, and hence the satellite will probe all local times during the course of a half year. An inclination of $i = 97.15^\circ$ (as for the Magsat satellite) yields an orbit plane which is fixed with respect to local time, denoted as a sun-synchronous orbit. The left part of Figure 1 illustrates the orbit geometry; the right part shows the ground track for 24 hours of Magsat observations.

Since the satellite moves and changes direction, it is essential to measure position and attitude of the magnetometer with high-precision. To obtain the magnetic field with an accuracy of 1 nT, the position must be known within 35 m, a goal which is easy to obtain with GPS receivers. Although induction studies can be performed with measurements of the magnetic field intensity $F = |\mathbf{B}|$ alone, using vector data is easier and gives more reliable results. This requires a high-precision attitude determination since an error of 4 arcseconds corresponds to an error in the magnetic field components of about 1 nT. Only star cameras are able to measure the attitude this accurately. Many satellites carry magnetometers, but their poor attitude determination means their data cannot be used for induction studies. Until now, only one high-precision vector satellite has flown, namely the Magsat satellite in 1979/80. Table I summarizes some parameters for Magsat as well as forthcoming missions. The attitude of Magsat is assumed to be known within ± 20 arcseconds (which corresponds to an error in the magnetic vector field components of about ± 5 nT) whereas the attitude error for the upcoming satellites Ørsted, SAC-C/MMP and Champ is expected to be only 2–5 arcseconds.

The satellite height is important insofar as only a low altitude allows for analyzing small scale structures. Measuring the magnetic field from an altitude h corresponds roughly to averaging over an area of this dimension. Hence a larger altitude might even be helpful for studying the global or regional conductivity

structure, since this corresponds to averaging over distorting local conductivity anomalies. Satellites usually fly in elliptical orbits, which results in an altitude range rather than one fixed altitude, again complicating the estimation of transfer functions (an exception is the satellite SAC-C/Ørsted-2 with its constant altitude of 702 ± 5 km, cf. Table I).

The magnetic field $\tilde{\mathbf{B}}_{\text{obs}}(t)$ measured by a satellite contains contributions from the core and the crust, as well as from current systems in the ionosphere and magnetosphere (and their induced contributions, of course). It is necessary to remove the core and crustal fields prior to an induction analysis because the measurements are made from a moving platform and the spatial changes of the core and crustal fields would be misinterpreted as temporal changes. This is done by subtracting model field values $\tilde{\mathbf{B}}_{\text{mod}}$. The residual field $\tilde{\mathbf{B}} = \tilde{\mathbf{B}}_{\text{obs}} - \tilde{\mathbf{B}}_{\text{mod}}$ then consists of ionospheric and magnetospheric contributions plus their induced counterparts. The transfer functions obtained from satellite data will be misleading if ionospheric currents are present, and hence these must be removed, too (or assumed to be absent). However, one should keep in mind that the core and crustal field models may be contaminated by external and induced contributions, and especially they may contain contributions due to anomalous induction.

In the following, $\tilde{\mathbf{B}}(t)$ is the time series of the magnetic residual field and is assumed to contain only magnetospheric contributions (which are of external origin) and their induced (internal) counterparts. A tilde above a value, like $\tilde{\mathbf{B}}(t)$, indicates that the quantity is a time series; its Fourier component is denoted without the tilde, like $\mathbf{B}(\omega)$. For the Fourier transformation a time dependence $\propto e^{i\omega t}$ is taken.

It is assumed that there are no electric currents at satellite altitude, and hence each Fourier component of the magnetic field residual $\mathbf{B}(\omega) - \text{grad } V(\omega)$ can be derived from a scalar magnetic potential V which is approximated by a spherical harmonic expansion:

$$V(r, \vartheta, \lambda, \omega) = a \sum_{n=1}^N \sum_{m=-n}^m \left[\epsilon_n^m(\omega) \left(\frac{r}{a}\right)^n + \iota_n^m(\omega) \left(\frac{a}{r}\right)^{n+1} \right] P_n^m(\cos \vartheta) e^{im\lambda}. \quad (1)$$

ϵ_n^m and ι_n^m are the complex expansion coefficients of the external and internal parts of the potential at frequency ω ; (r, ϑ, λ) are spherical coordinates with $a = 6371.2$ km as the mean Earth's radius and ϑ and λ as geographic (or geomagnetic) colatitude and longitude; P_n^m are the associated Legendre functions. The magnetic field components follow from this potential expansion as

$$\begin{pmatrix} B_r \\ B_\vartheta \\ B_\lambda \end{pmatrix} = \begin{pmatrix} -\sum_{n,m} \left[n\epsilon_n^m \left(\frac{r}{a}\right)^{n-1} - (n+1)\iota_n^m \left(\frac{a}{r}\right)^{n+2} \right] P_n^m e^{im\lambda} \\ -\sum_{n,m} \left[\epsilon_n^m \left(\frac{r}{a}\right)^{n-1} + \iota_n^m \left(\frac{a}{r}\right)^{n+2} \right] \frac{dP_n^m}{d\vartheta} e^{im\lambda} \\ -\sum_{n,m} \left[\epsilon_n^m \left(\frac{r}{a}\right)^{n-1} + \iota_n^m \left(\frac{a}{r}\right)^{n+2} \right] \frac{im}{\sin \vartheta} P_n^m e^{im\lambda} \end{pmatrix}. \quad (2)$$

The expansion coefficients ι_n^m and ϵ_n^m can be estimated from a set of measurements of the magnetic field components, for instance in a least squares sense. Note that ι_n^m and ϵ_n^m refer to ground ($r = a$) even if the magnetic measurements are taken at the (fixed) altitude h or even within a whole range of altitudes. In the latter case, a *combined simultaneous* analysis of all three magnetic components is necessary for the separation of external and internal contributions. However, when analyzing data from one fixed altitude (like ground based data), this separation is possible from separate analyses of the horizontal vector $\mathbf{B}_H = (B_\vartheta, B_\lambda)$ and of the vertical component B_r , respectively.

Until now, all attempts to estimate the conductivity-depth profile from satellite data have relied on the assumption that the external (inducing) source is of magnetospheric origin with a spatial structure described by the spherical harmonic $P_1^0 = \cos \vartheta$ alone, where ϑ is geomagnetic colatitude. In this case the magnetic components (in the geomagnetic coordinate system) are given by

$$\begin{pmatrix} B_r \\ B_\vartheta \\ B_\lambda \end{pmatrix} = \begin{pmatrix} \left[-\epsilon_1^0 + 2\iota_1^0 \left(\frac{a}{r}\right)^3 \right] \cos \vartheta \\ \left[+\epsilon_1^0 + \iota_1^0 \left(\frac{a}{r}\right)^3 \right] \sin \vartheta \\ 0 \end{pmatrix}. \quad (3)$$

According to Gauss, this allows the separation of external (ϵ) and internal (ι) parts. Studies with observatory data have shown that the inclusion of more spherical harmonics significantly increases the accuracy of the transfer functions (Olsen, 1998). Oraevsky et al. (1993a, 1993b) used the Magsat data set and determined source structure models with more terms than just P_1^0 but the additional terms were considered not to be resolvable. It is believed that more coefficients can be resolved with longer time-series from future satellites, and especially from a joint analysis of data from more than one satellite, and in combination with ground observations.

3. Response Functions for Induction Studies With Satellite Data

Two methods are used to study the electrical conductivity of the Earth's interior using natural magnetic variations in the period range hours to months. In the first, known as the potential method, a spherical harmonic analysis of the geomagnetic field is performed, and the Q -response (the ratio of induced to external expansion coefficient) is determined. This approach treats the magnetic field in the spherical harmonic spectral domain. In the second approach, known as the geomagnetic depth sounding method, the C -response (the ratio of vertical component to the spatial derivative of the horizontal components) is the basic transfer function. It is derived in the spatial domain, which makes the detection of lateral conductivity inhomogeneities easier, at least for small deviations from a 1-D conductivity structure (1-D conductivity means that the conductivity σ depends only on the radius). The

TABLE II
Response functions used in satellite studies

At ground ($r = a$)	At satellite height ($r = a + h$)
$Q_n = \frac{i^n}{\epsilon_n^m}$	
$W_n(a) = \frac{B_r(a)}{B_\vartheta(a)} \frac{dP_n^m/d\vartheta}{P_n^m}$	$W_n(r) = \frac{B_r(r)}{B_\vartheta(r)} \frac{dP_n^m/d\vartheta}{P_n^m}$
$W_1(a) = \frac{B_r(a)}{B_\vartheta(a)} \tan \vartheta$	$W_1(r) = -\frac{B_r(r)}{B_\vartheta(r)} \tan \vartheta$
$C_n(a) = \frac{a}{n+1} \frac{1 - \frac{n+1}{n} Q_n}{1 + Q_n}$	$C_n(r) = \frac{r}{n+1} \frac{(\frac{r}{a})^{2n+1} - \frac{n+1}{n} Q_n}{(\frac{r}{a})^{2n+1} + Q_n}$ $= C_n(a) + \left[1 - n(n+1) \left(\frac{C_n(a)}{a} \right)^2 \right] h + \dots$
$C_1(a) = \frac{a}{2} \frac{1 - 2Q_1}{1 + Q_1}$ $= \frac{a}{2} W_1(a)$	$C_1(r) = \frac{r}{2} \frac{(\frac{r}{a})^3 - 2Q_1}{(\frac{r}{a})^3 + Q_1}$ $= \frac{r}{2} W_1(r)$
$\rho_a(a) = \omega\mu_0 C(a) ^2$	$\rho_a(r) = \omega\mu_0 C(r) ^2$
$\phi(a) = \frac{\pi}{2} + \arg\{C(a)\}$	$\phi(r) = \frac{\pi}{2} + \arg\{C(r)\}$

C -response is closely related to the magnetotelluric impedance Z and to apparent resistivity ρ_a and phase ϕ according to Schmucker, 1987.

$$Z = i\omega\mu_0 C \quad (4)$$

$$\rho_a = \omega\mu_0 |C|^2 \quad (5)$$

$$\phi = \pi/2 + \arg\{C\} \quad (6)$$

The two methods are well proven for the analysis of ground data (for a discussion of the methods, see, for instance, Schmucker 1970, 1985a, 1987, and Parkinson and Hutton 1989), but when applied to satellite data, the effects of the satellite altitude and its variation must be considered carefully. Table II summarizes often used response functions and their dependences on radius. Responses referring to the satellite orbit are denoted as $C_n(r)$, while those referring to ground are denoted as $C_n(a)$ or simply as C_n since the Earth's radius a is the preferred reference radius. The case with $n = 1$ is of special interest for induction studies in the period range between 2 days and one month (because the source geometry is dominated by P_1^0), and hence is listed separately.

3.1. POTENTIAL METHOD AND Q -RESPONSE

The first approach relies on the separation of external (inducing) and internal (induced) contributions using a spherical harmonic expansion. The transfer function used is the (complex) Q -response, which is the ratio of the internal to external

expansion coefficients for a specific degree, order and frequency. This definition is especially useful for the case of a spherically symmetric (1-D) conductivity distribution. In this case each external coefficient induces only one internal coefficient (of the same degree n and order m) and their ratio Q is independent on m

$$l_n^m = Q_n \epsilon_n^m \quad (7)$$

(but depends, of course, on frequency ω). In the general case of a 3-D conductivity (σ is a function of both vertical and horizontal coordinates), each external coefficient ϵ_n^m induces a whole spectrum of internal coefficients l_n^m , and hence Equation (7) has to be replaced with the more general relationship

$$l_n^m = \sum_{l,k} q_{ln}^{km} \epsilon_l^k. \quad (8)$$

However, for the case of weak deviations from the 1-D case (small horizontal conductivity gradients in the sense $|\partial\sigma/\partial x|, |\partial\sigma/\partial y| \ll \sigma/p = \sqrt{\frac{2\sigma}{\omega\mu_0}}$ where $p = \sqrt{\frac{2}{\omega\mu_0\sigma}}$ is the skin depth), Equation (7) can still be used.

Q as defined in Equation (7) refers to the Earth's radius $r = a$ and is related to the (complex) ground C -response as

$$C_n(a) = \frac{a}{n+1} \frac{1 - \frac{n+1}{n} Q_n}{1 + Q_n} \quad (9)$$

C_n has – contrary to the transfer functions Q_n and W_n (defined below) but similarly to ρ_a and ϕ – the important property of being asymptotically independent of the source dimensions: $C_n \rightarrow C$ for $|C| \ll a/n$. Since this condition is fulfilled for the periods used in satellite induction studies (shorter than one month or so) and low degree spherical harmonics ($n \lesssim 3$), the subscript n will be dropped in the following for C , ρ_a and ϕ .

The potential method is the classical approach for studying mantle conductivity and was used for the first time at the end of the last century. Since ϵ_n^m and l_n^m refer to the Earth's radius a , the Q -responses do so as well. Hence results obtained with satellite data are directly comparable to those found from ground data, which is an advantage of the potential method. A disadvantage is that the response function is obtained in the spherical harmonic domain. Conductivity anomalies affect therefore all expansion coefficients and hence all responses in a complicated way. However, studying large scale conductivity differences is still possible, for instance, by analyzing only the data for which the satellite was over a selected region, thus obtaining responses for this specific region.

3.2. GRADIENT METHOD AND C -RESPONSE

In the second approach, the C -response is the basic transfer function. It is defined as (Schmucker, 1985b)

$$C = \frac{B_r}{\partial B_r / \partial r} = -\frac{B_r}{\mathcal{G}} \quad (10)$$

(here $\nabla \cdot \mathbf{B} = 0$ is used) with

$$\begin{aligned} \mathcal{G}(\omega, r, \vartheta, \lambda) &= \nabla_{\mathbf{H}} \cdot \mathbf{B}_{\mathbf{H}} \\ &= \frac{1}{r \sin \vartheta} \left[\frac{\partial}{\partial \vartheta} (\sin \vartheta B_{\vartheta}) + \frac{\partial B_{\lambda}}{\partial \lambda} \right] \end{aligned} \quad (11)$$

being the divergence of the horizontal vector $\mathbf{B}_{\mathbf{H}} = (B_{\vartheta}, B_{\lambda})$.

If the source field can be described by a single spherical harmonic and the conductivity is assumed to be 1-D, this yields the classical Z/H -method (Banks, 1969) which allows for the estimation of the C -response from magnetic measurements at a single site. Assuming a P_1^0 source, combination of Equations (10) and (11) yields

$$C(r, \vartheta, \lambda) = \frac{r}{2} W_1(r, \vartheta, \lambda) = -\frac{r \tan \vartheta}{2} \frac{B_r(r, \vartheta, \lambda)}{B_{\vartheta}(r, \vartheta, \lambda)} \quad (12)$$

where

$$W_1(r, \vartheta, \lambda) = -\frac{B_r(r, \vartheta, \lambda)}{B_{\vartheta}(r, \vartheta, \lambda)} \tan \vartheta \quad (13)$$

is Bank's W -response for degree $n = 1$ and frequency ω (Banks, 1969).

Note that this method yields the response $C(r)$ at satellite height, but transformation to the corresponding ground response $C(a)$ is straightforward if the space between ground and satellite is nonconducting. Neglecting the sphericity of the Earth (that is using the Flat-Earth approximation, $a \rightarrow \infty$), this transformation is given by

$$C(a) = C(r) - h. \quad (14)$$

When the Earth's sphericity is taken into account, the transformation can be performed by first calculating Q_n using

$$Q_n = \frac{n}{n+1} \frac{1 - (n+1) \frac{C_n(r)}{r}}{1 + n \frac{C_n(r)}{r}} \left(\frac{r}{a} \right)^{2n+1} \quad (15)$$

followed by a transformation $Q_n \rightarrow C_n(a)$ by means of Equation (9). To first order in height h this yields

$$C_n(a) = C_n(r) - \left[1 - n(n+1) \left(\frac{C(a)}{a} \right)^2 \right] h + \dots$$

(in which the Flat-Earth transformation Equation (14) is recognized for $a \rightarrow \infty$).

If the magnetic data are acquired within a range of altitudes rather than at one fixed altitude, the equations to be used are more complicated. It is necessary to refer the response to one specific radius, and choosing the Earth's radius yields the ground response $C(a)$ directly:

$$C(a, \vartheta, \lambda) = \frac{a W_1(r, \vartheta, \lambda) \left(\left(\frac{a}{r} \right)^3 + 2 \right) + 2 \left(\left(\frac{a}{r} \right)^3 - 1 \right)}{2 W_1(r, \vartheta, \lambda) \left(\left(\frac{a}{r} \right)^3 - 1 \right) + \left(2 \left(\frac{a}{r} \right)^3 + 1 \right)}. \quad (16)$$

This equation reduces to Equation (12) for $r = a$. However, it depends nonlinearly on W for $r \neq a$, which complicates the estimation of $C(a)$ when data from different altitudes (and hence different r) are analyzed together.

Neglecting the height variation and using Equation (12) with a fixed mean radius r yields a larger statistical error of the response function. This effect depends – besides of the size of the height variation – on the mean height \bar{h} , the degree n , and the value of C . A look at the altitude variation of the Magsat satellite might be helpful to understand the impact of neglecting it. The mean altitude of Magsat decreased from roughly 550 km in November 1979 to roughly 350 km in May 1980; 50% (75%) of the data were acquired at altitudes 430 ± 60 km (430 ± 75 km), and 95% of the data belong to the altitude range 430 ± 100 km. However, one should keep in mind that this height variation is not random, but rather systematic.

In the Flat-Earth approximation, the relative error on C due to ignoring a radial variation δr is $\left| \frac{\delta C(r)}{C(r)} \right| = \left| \frac{\delta r}{C(r)} \right| = \left| \frac{\delta r}{C(a)+\bar{h}} \right|$. A radial variation $\delta r = 100$ km, a mean altitude $\bar{h} = 430$ km and a ground response of $C(a) = 610 - 250i$ km (which is a typical value for a period of $T = 1$ day) yields a relative error of $\left| \frac{\delta C(r)}{C(r)} \right| \approx 9\%$; a ground response of $C(a) = 890 - 290i$ km (corresponding to a period of $T = 10$ days) gives a relative error of 7%. The relative errors of the apparent resistivity ρ_a are twice as much as those values, and we can conclude that neglecting the height variation of the Magsat satellite contributes up to 20% to the uncertainty of ρ_a .

To circumvent the difficulties connected with the height variation, it is more convenient to use the Q -response rather than the C -response. Assuming again a source field entirely consisting of P_1^0 , time series of the external and internal parts can be derived directly from the residual magnetic field components \tilde{B}_r and \tilde{B}_ϑ :

$$\tilde{\tau}(t) = \frac{1}{3} \left(\frac{r}{a} \right)^3 \left(\frac{\tilde{B}_\vartheta(t)}{\sin \vartheta} + \frac{\tilde{B}_r(t)}{\cos \vartheta} \right) \quad (17)$$

$$\tilde{\epsilon}(t) = \frac{1}{3} \left(2 \frac{\tilde{B}_\vartheta(t)}{\sin \vartheta} - \frac{\tilde{B}_r(t)}{\cos \vartheta} \right). \quad (18)$$

Due to the factor $(r/a)^3$ and the division of \tilde{B}_ϑ with $\sin \vartheta$ and \tilde{B}_r with $\cos \vartheta$, respectively, the quantities $\tilde{\iota}$ and $\tilde{\epsilon}$ are independent of latitude and radius for a given magnetospheric source field (although \tilde{B}_ϑ and \tilde{B}_r of course depend on latitude and radius). Hence it is possible to average them. Unfortunately, such an approach is not possible if the source field contains more than one spherical harmonic (unless an a priori value of their relative contributions is assumed). However, Equations (17) and (18) should not be used for averaging over latitudes, since the right hand sides are no longer gaussian distributed, even if the distributions of \tilde{B}_ϑ and \tilde{B}_r are gaussian, because of the weights $1/\sin \vartheta$ and $1/\cos \vartheta$.

Instead of that, it is more convenient to apply the potential method and estimate the expansion coefficients in a least-squares sense, even if data of selected regions only (for instance in the northern hemisphere only) are used. Of course this requires a careful investigation of the stability of the inversion, but the mentioned complications connected with the altitude variations of the satellite speak in favor of the potential method for induction studies using satellite data.

3.3. EFFECT OF IONOSPHERIC CONDUCTIVITY

Satellite data are usually acquired at heights above 350 km, and hence the conductivity of the ionosphere beneath the satellite influences the transfer functions since they do not probe solely the conductivity of the Earth's interior. This effect is discussed, for instance, by Didwall (1984) and Rotanova et al. (1995) and has been found to be negligible. This becomes clear when treating the ionosphere as a thin sheet of conductance τ . The C -responses just above (C^+) and just below (C^-) this sheet are connected according to

$$\frac{1}{C^+} = \frac{1}{C^-} + i\omega\mu_0\tau$$

(Equation (9) of Schmucker 1987). Ionospheric conductivity is extremely variable as a function of local time, latitude and other parameters but a typical upper limit for the height integrated conductivity in the altitude range 90–300 km is $\tau \lesssim 50$ S. Assuming a period of $T = 1$ day and $|C| = 600$ km, the quantity $\omega\mu_0\tau = 5 \cdot 10^{-9} \text{ m}^{-1}$ is much smaller than $1/|C| = 1.7 \cdot 10^{-6} \text{ m}^{-1}$ and hence the influence of the ionospheric conductivity can be neglected.

4. Results of Induction Studies With Satellite Data

4.1. EARLY INDUCTION STUDIES

The first induction studies using satellite data were performed with measurements from the KOSMOS-321 satellite, which measured the magnetic total intensity at noon and midnight, respectively, at altitudes between 250 and 400 km. Combining

ground and satellite observations of the Equatorial Electrojet, Dolginov (1972) estimated the depth of an infinite conductor, which is assumed to approximate the Earth's conductive basement, to 123 km. This is only half the value found from ground data alone (for a period of about 1 day). Van'yan et al. (1975) reanalyzed the data and pointed out that the width of the Equatorial Electrojet is not constant (as assumed by Dolginov (1972)) but has to be estimated separately for every orbit. They also account for the finite conductivity of the mantle, and found depths of the conducting basement of 250–350 km in better agreement with the results from other studies.

The first global induction study with satellite data was initially considered by Langel (1975) using data of the POGO satellites which operated during the years 1965 to 1971 in the altitude range between 400 km and 1500 km. However, estimating response functions was complicated because the satellites only measured the magnetic field intensity but not its vector components. Assuming a P_1^0 source for the potential of fields produced by magnetic storms,

$$\tilde{V}(r, \vartheta, \lambda, t) = a \left[\tilde{t}_1^0(t) \left(\frac{r}{a} \right) + \tilde{\epsilon}_1^0(t) \left(\frac{a}{r} \right)^2 \right] \cos \vartheta, \quad (19)$$

Langel (1975) solved for the time series $\tilde{t}_1^0(t)$ and $\tilde{\epsilon}_1^0(t)$ by analyzing the residual field during strong magnetic storms (after subtracting a main field model) and found ratios $\tilde{Q}_1(t) = \tilde{t}_1^0(t)/\tilde{\epsilon}_1^0(t)$ between 0.22 and 0.41 in agreement with studies based on observatory data.

Langel and Estes (1985) used Magsat vector measurements to estimate the geomagnetic main field simultaneously with a magnetospheric field approximated by a P_1^0 source (in geographic rather than geomagnetic coordinates) plus its induced counterpart. They assumed a linear dependency of the dipole coefficients on the *Dst* index (in units of nT); hence the time-dependence of their model is given by that of the *Dst* index. For the external coefficient they found $\tilde{\epsilon}_1^0(t) = 18.4 \text{ nT} - 0.63 \cdot \text{Dst}(t)$; the corresponding internal part was $\tilde{t}_1^0(t) = -29991.6 \text{ nT} - 0.17 \text{Dst}(t)$. The time independent internal term describes the axial dipole coefficient $g_1^0 = -29991.6 \text{ nT}$ of the main field (for epoch 1980) whereas the time independent external part of 18.4 nT represents a constant contribution from the magnetospheric ring current. The chosen parameterization does not allow for a time lag between induced and inducing fields (since the time dependency is given explicitly by the *Dst* index) and hence corresponds to the model of a perfect conductor at a specific depth. The ratio of induced to inducing contributions is

$$\tilde{Q}_1 = \frac{-0.17}{-0.63} = +0.270,$$

which corresponds to a perfect conductor at a depth of 1138 km. This is in reasonable agreement with other induction studies (see the compilation in Table 9 of Schmucker 1985a), if one considers the typical period of storm variations to be several days.

4.2. GLOBAL STUDIES WITH POGO AND MAGSAT DATA

Further studies by Didwall and Langel (1976, 1977) and Didwall (1980, 1981, 1984) treated the problem in the frequency domain, which allows for the probing of the conductivity-depth profile of the mantle. Didwall (1984) presents results obtained from an analysis of POGO measurements of eight magnetic storms. For each of these storms, time series of \tilde{t}_1^0 and $\tilde{\epsilon}_1^0$ were determined and transformed into the frequency domain. After “stacking” the spectra, $Q_1(\omega) = \iota_1^0(\omega)/\epsilon_1^0(\omega)$ was estimated for 9 periods between 12 and 120 hours. Squared coherency was rather high (above 0.9) but decreased for periods shorter than 24 hours. Didwall (1984) considered the problem of up- or downward biased estimates due to improper assumptions about the relative noise in ι_1^0 and ϵ_1^0 . The results presented in her Table 1 have been transformed to C -response values assuming equal noise in ι_1^0 and ϵ_1^0 (which implies using the geometric mean rather than the arithmetic mean as was done in Equation (11) of Didwall (1984)) and are shown in Figure 2. Two sets of observatory results are also displayed. Constable (1993) derived a global response by averaging the results of Schultz and Larsen (1987) and Roberts (1984), which were obtained using the Z/H -method assuming a P_1^0 -source. Olsen (1998) used more than one spherical harmonic (up to 120) and obtained mean responses by averaging the results from European observatories. The lines in Figure 2 represent the responses of the D^+ models (Parker, 1980) fitted to the results of Constable (1993) and Olsen (1998), respectively.

Despite the large errors, the POGO data clearly sample the average conductivity of the mantle in a way not possible with observatory data on continents. This was the first attempt to derive the conductivity-depth structure of the Earth using satellite data and demonstrated the possibility of probing the Earth’s conductivity from space.

Induction studies using Magsat vector data considering the time lag between inducing and induced contributions have been reported in a series of papers. Orlovsky et al. (1992a, 1992b, 1993a, 1993b) analyzed Magsat data covering the whole Earth using two approaches:

In the first approach they applied Equation (19) to Magsat evening data equatorward of 65° geomagnetic latitude and estimated the time series $\tilde{\epsilon}_1^0(t)$ and $\tilde{t}_1^0(t)$. After low-pass filtering to remove the influence of ionospheric S_q currents, the time series were Fourier analyzed to obtain $\iota_1^0(\omega)$ and $\epsilon_1^0(\omega)$ in the period range between 30 and 190 hours, and finally $Q_1(\omega) = \iota_1^0(\omega)/\epsilon_1^0(\omega)$ was estimated. The authors derived transfer functions with this approach by analyzing time series of the whole Magsat lifetime of about 6 months, as well as by using data of 20 geomagnetic storms only. However, these results have not been published.

In the second approach, they used Magsat evening data at $\pm 45^\circ$ geomagnetic latitude from which they derived time series of Bank’s transfer function $\tilde{W}_1(r) = \tan \vartheta \tilde{B}_r / \tilde{B}_\vartheta$. A transformation to the spectral domain yielded the responses $W_1(r)$, which finally were converted to apparent resistivity $\rho_a(r) =$

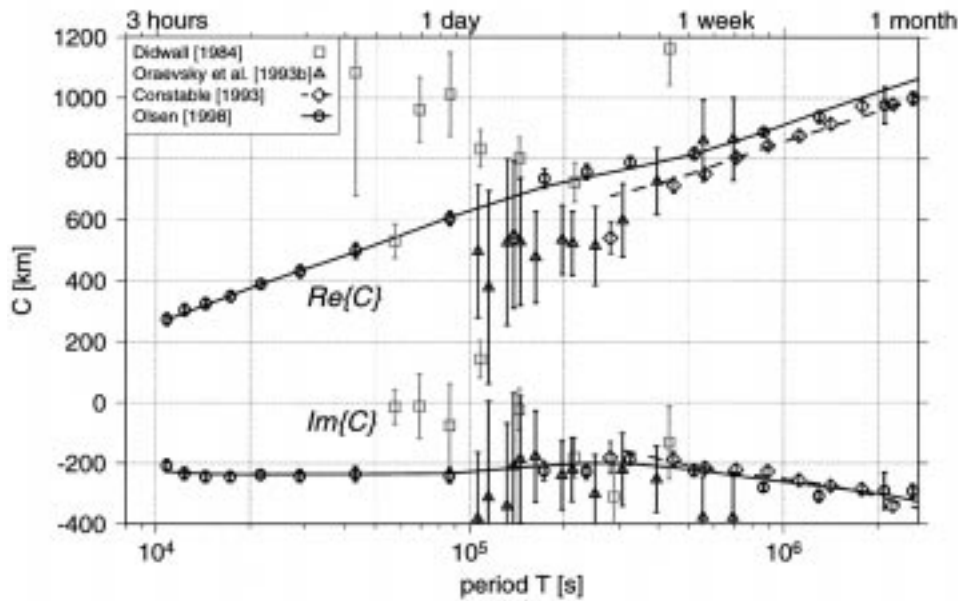


Figure 2. C -responses from magnetic data obtained by the POGO satellites (after Didwall, 1984), by Magsat (after Oraevsky et al., 1993b) and using worldwide distributed observatories (after Constable, 1993), respectively European observatories (after Olsen, 1998). The lines represent the responses of the D^+ models fitted to the results of Constable (1993) and Olsen (1998), respectively.

$\omega\mu_0\frac{r^2}{4}|W_1(r)|^2$ and phase $\phi(r) = \pi/2 + \arg\{W_1(r)\}$. Note that r should be the radius of the satellite observations, not the Earth's radius a , as was done incorrectly by Oraevsky et al. (1992a, 1993a, 1993b). This implies that the apparent resistivities presented in Table 2 of Oraevsky et al. (1993b) must be multiplied by a factor of $\left(\frac{a+\bar{h}}{a}\right)^2 = 1.14$ (assuming a mean Magsat height of $\bar{h} = 430$ km). However, even after applying this factor, the responses still refer to satellite height. The corresponding ground responses presented in Figure 2 have been derived using Equations (15) and (9).

The Magsat responses are much more noisy (the mean relative error is 23%) than the observatory responses (relative error: 3%), which presumably is due to the shorter time series of the satellite study. Satellite responses at periods near 1 day are probably contaminated by ionospheric Sq contributions. With this in mind, the agreement between satellite and ground responses is reasonable. The Magsat results are close to those of Constable (1993); whereas the real part of C is larger for the responses obtained from European observatories. This might be due to the fact that the latter is a regional response, as opposed to the global responses of the other studies.

4.3. REGIONAL STUDIES WITH MAGSAT DATA

A geomagnetic sounding for different longitudes has been reported by Rotanova et al. (1995) and Semenov et al. (1997). They subdivided the values of the time series $\tilde{W}_1(r)$ defined in the previous section into three longitude sectors: a Pacific sector (between 170° and 230° geographic longitude), an American Sector (240°–310° longitude) and an European-African sector (350°–60° longitude). Of course the resulting three time series have gaps (when the satellite was over other regions), and the authors deal with this in two ways: (a) the missing values are spline interpolated; and (b) the values of one day are averaged to obtain new time series with a sampling rate of one day. After transforming into the frequency domain, response functions are estimated using Equation (12).

It turns out that the results for the American and the Pacific regions are rather similar, whereas those for the European-African region differ. The authors attribute this to the distribution of continents and oceans, and they merged the American and the Pacific results to obtain “oceanic” values in contrast to the European-African responses, which they denote “continental”. The left part of Figure 3 shows their results. “Oceanic” and “continental” apparent resistivities differ most at shorter periods, indicating a possible influence of induction in the oceans. Conductivity models consistent with these observations are presented in the right part of the Figure, and the model responses are shown in the left part by lines. The models differ only in the conductance of the top layer (oceans: 20 kS, continents: 0.1 kS), reflecting the presence of seawater. Induction in the oceans with a realistic land-ocean distribution has been carried out by Kendall and Quinney (1983), Takeda (1985), Winch (1989) and Kuvshinov et al. (1999). They found that ocean induction is negligible for periods longer than a few days. (See also Section 5 for the effect of the conducting seawater on the estimation of transfer functions using satellite data.)

Latitudinal differences of the responses are mentioned by Semenov et al. (1997) who pointed out that time series of the radial component \tilde{B}_r in the southern hemisphere (–45° geomagnetic latitude) have larger amplitudes as compared to the northern hemisphere (+45° geomagnetic latitude) while the time series of the horizontal component \tilde{B}_θ are rather similar. They discuss the possibility that this is due to ionospheric Sq currents, which are expected to be weaker in the northern hemisphere during northern winter.

4.4. A NEW ANALYSIS OF MAGSAT DATA

In the following I present new results obtained from the Magsat data set, regarding both global and regional soundings. The data set consists of 6 months of data (November 3, 1979 to May 6, 1980), corresponding to 3000 orbits, with a sampling rate of 5 seconds. Both the evening and morning parts of the orbits are used but results are only presented for the evening data, since they are more consistent. The following steps are applied to estimate responses. The GSFC(12/83) field model is

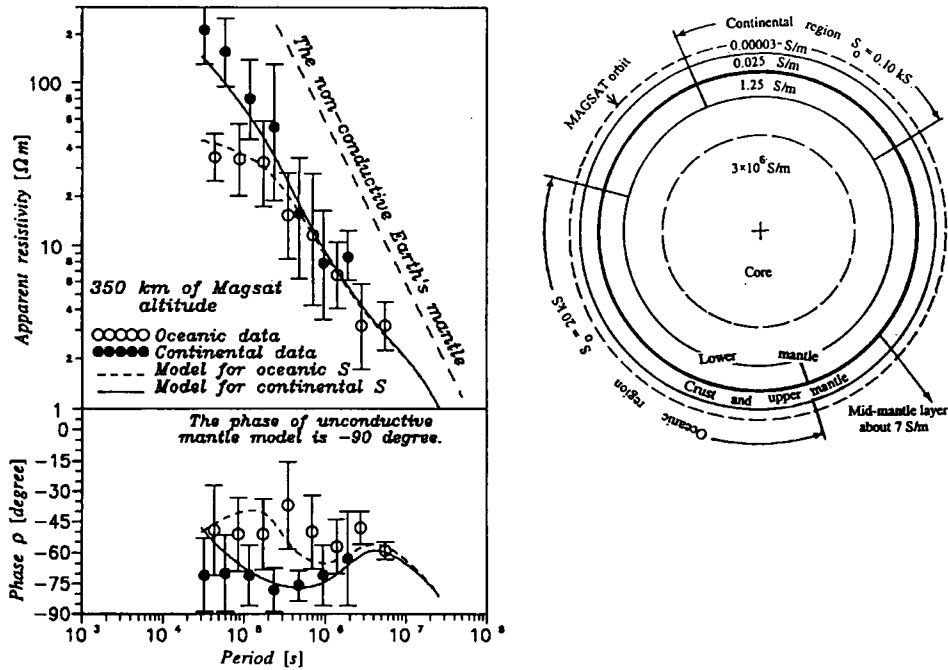


Figure 3. Apparent resistivity $\rho_a(r)$ and phases $\phi(r)$ obtained from a regional sounding using Magsat data (left, after Semenov et al. (1997)). Note that the responses refer to satellite height rather than ground. The lines represent the responses of the models shown in the right part. In these models, the upper mantle extends to a depth of 670 km, the mid-mantle to a depth of 770 km, and the lower mantle to a depth of 1600 km.

subtracted from all observations. This model describes the main field up to degree and order 13 and a linear secular variation up to degree and order 8. Then, time series of the external and internal contributions are estimated from the evening parts of each of the about 3000 orbits assuming a P_1^0 source. In doing so, the coefficients $\tilde{\epsilon}_1^0$ and $\tilde{\tau}_1^0$ of Equation (19) were estimated in a least squares sense for each orbit separately. Formal errors are estimated, too; typical values for $\delta\tilde{\epsilon}_1^0$ and $\delta\tilde{\tau}_1^0$ are between 0.3 and 1 nT.

To study regional differences (especially those connected with the ocean/continent distribution) the data were binned according to various criteria. I will outline the method for a data subdivision into a northern and a southern set, but results obtained from a selection according to oceanic/continental regions will be presented later.

Two pairs of time series are derived: one pair, denoted as $\tilde{\tau}_N$ and $\tilde{\epsilon}_N$, by using data from the northern hemisphere at geomagnetic latitudes $15^\circ < \varphi < 50^\circ$ only, and one pair from southern hemisphere data ($-50^\circ < \varphi < -15^\circ$) only, denoted as $\tilde{\tau}_S$ and $\tilde{\epsilon}_S$. These time series have a sampling rate of 90 minutes, since this is the orbit period of Magsat. Gaps of fewer than 6 orbits were interpolated by splines.

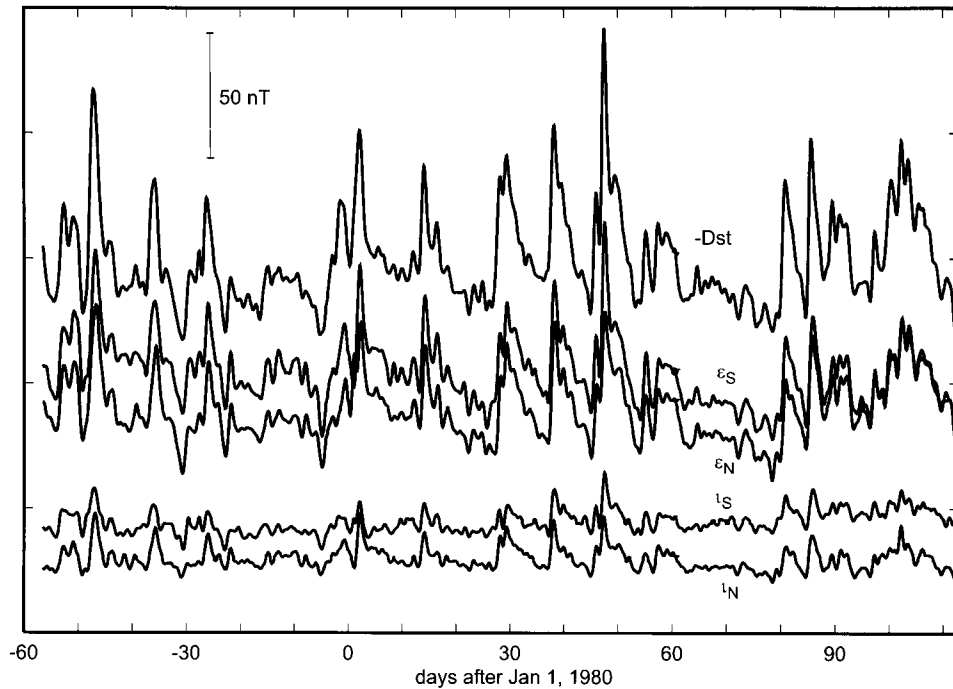


Figure 4. Time series of external and internal coefficients assuming a P_1^0 -source obtained from northern and southern hemisphere Magsat data, respectively. For comparison, the Dst -index is shown, too. A low-pass filter with a cut-off period of 30 hours has been applied to all five time series.

Figure 4 shows the four time series together with the Dst index. (For this plot, a low-pass filter with a cut-off period of 30 hours was applied to remove the diurnal variation, which is probably mainly caused by ionospheric Sq currents.) There is a good correlation between $\tilde{\epsilon}_N$ and $\tilde{\epsilon}_S$, which confirms the P_1^0 assumption. If in addition the Earth's conductivity is 1-D (and there are no ionospheric currents), one would expect a similar good correlation between \tilde{I}_S and \tilde{I}_N . This, however, seems not to be the case: the variations of \tilde{I}_S are of smaller amplitudes than those of \tilde{I}_N .

Figure 5 shows the quadratic spectra and the squared coherencies of the time series. They are almost flat for periods shorter than 2 days at a level of $\approx 1 \text{ nT}^2$ for the external coefficients and $\approx 0.2 \text{ nT}^2$ for the internal coefficients. There are pronounced peaks at the period $T = 1$ day of similar magnitude in the external and internal contributions. This indicates that the internal contribution is not entirely induced (in which case one would expect $\iota/\epsilon \approx 0.4$). Ionospheric contributions, especially from the Sq currents, which are of internal origin as seen from the satellite, are probably the main source for the internal signal at $T = 1$ day. Hence the assumption that internal contributions are of purely induced origin is violated and the transfer functions for this period should not be interpreted in terms of mantle

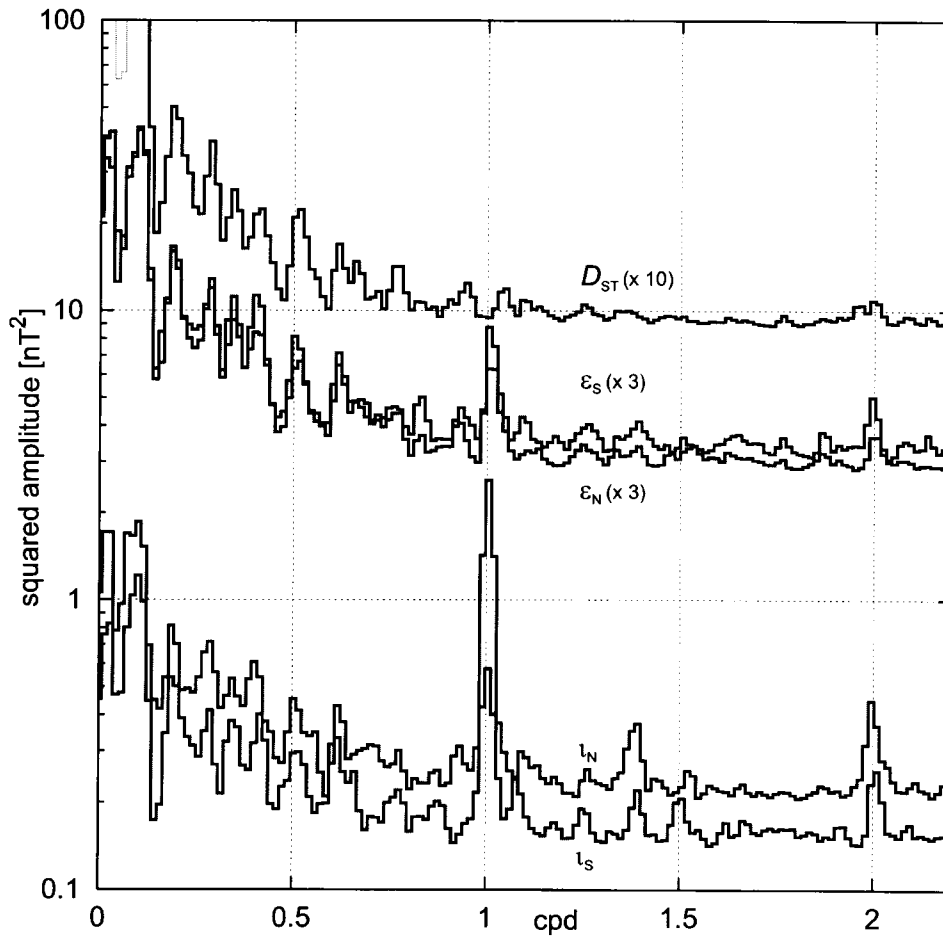


Figure 5. Quadratic spectra of the time series of Figure 4 (prior to the low-pass filtering, however). The squared amplitude of ϵ is multiplied by a factor of 3, and that of Dst is multiplied by a factor of 10.

conductivity (see Section 6 on the use of ionospheric currents for induction studies). Magnetospheric current systems, especially the Chapman-Ferraro currents at the magnetopause, are probably responsible for the external signal at $T = 1$ day.

Each time series is split up into L segments of length T and the Fourier components corresponding to this period are estimated. Twelve values of T between 9 hours and 20 days (equally spaced in $\log T$) are chosen, and squared-spectra $\langle \epsilon \epsilon^* \rangle$, $\langle I I^* \rangle$ as well as cross-spectra $\langle \epsilon I^* \rangle$, $\langle I \epsilon^* \rangle$ are estimated for these 12 periods using a robust approach. ϵ^* is the complex conjugate of ϵ , and $\langle \dots \rangle$ denotes sum-

mation over all L realizations. Finally, upward and downward biased values of the Q -responses and squared coherency are estimated according to

$$Q^U = \frac{\langle \iota^* \rangle}{\langle \epsilon \iota^* \rangle} \quad (20)$$

$$Q^D = \frac{\langle \iota \epsilon^* \rangle}{\langle \epsilon \epsilon^* \rangle} \quad (21)$$

$$\text{coh}^2 = \frac{\langle \iota \epsilon^* \rangle \langle \epsilon \iota^* \rangle}{\langle \epsilon \epsilon^* \rangle \langle \iota \iota^* \rangle} = \frac{Q^D}{Q^U} \quad (22)$$

The downward biased estimate Q^D corresponds to the assumption of errors only in ι , whereas the upward biased estimate Q^U corresponds to the assumptions of errors only in ϵ . In an attempt to derive a value Q with minimal statistical bias, equal relative noise in ι and ϵ is assumed, which results in $Q = \sqrt{Q^D Q^U}$. The statistical error δQ is determined from

$$\left| \frac{\delta Q}{Q} \right|^2 = \frac{1 - \text{coh}^2}{\text{coh}^2} \frac{2}{2L' - 2} F_{2;2L'-2;1-\beta}^{-1} \quad (23)$$

where $F_{2;2L'-2;1-\beta}^{-1}$ is the inverse of the F distribution function with 2 and $2L' - 2$ degrees of freedom. L' is the effective number of data segments (that is the sum of the weights used in the robust approach), and the confidence level $(1 - \beta)$ is chosen to be $(1 - 0.32) = 0.68$. Details of this scheme can be found in Olsen (1998).

Four different transfer functions are estimated: $Q_N = \iota_N / \epsilon_N$ and $Q_S = \iota_S / \epsilon_S$ are the transfer functions between the external and induced coefficients in the northern and southern hemisphere, respectively. In addition to that, the transfer function ϵ_S / ϵ_N between the external coefficients of the two hemispheres as well as that between the internal coefficients, denoted as ι_S / ι_N , are derived.

Figure 6 shows these transfer functions and the corresponding coherencies. The upper left plot concerns ϵ_S / ϵ_N . The real part (squares) of the transfer function is close to unity; the imaginary part (triangles) is close to zero, indicating the similarity of the two time series. Squared coherency (circles connected with a line) is generally above 0.9, but drops dramatically at periods shorter than 2 days. The upper right plot shows the corresponding values for ι_S / ι_N , coh^2 is now only 0.7–0.8, and the transfer function is smaller than 1 at all frequencies, indicating smaller values of ι_S as compared to ι_N . The lower panel shows the transfer function Q_N (respectively Q_S) between the internal and external parts. Q_S , shown in the right bottom plot, is smaller than Q_N , (left bottom plot) indicating weaker induction in the southern hemisphere.

The upper part of Table III shows the result of this analysis as C -responses, apparent resistivities ρ_a and phases ϕ . The “global” values were obtained by taking

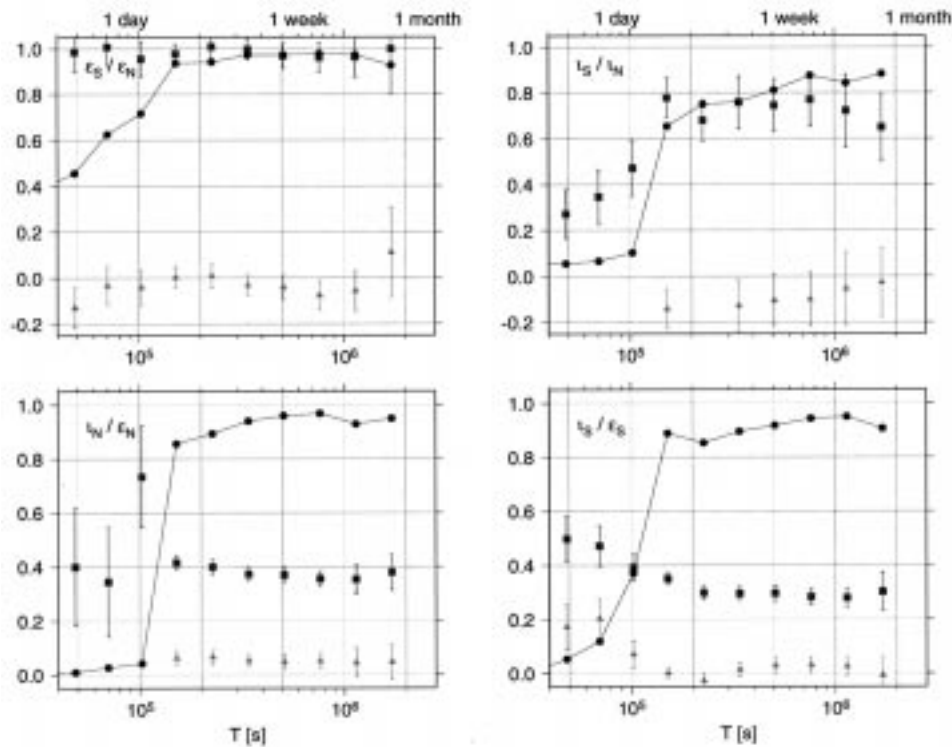


Figure 6. Transfer functions and squared coherencies of the time series. Real and imaginary parts of the transfer functions are shown with squares respectively triangles; the error bars refer to the 68% level. Squared coherencies are presented by circles.

all observations, regardless of whether they were obtained in the northern or in the southern hemisphere. Apparent resistivities and phases are plotted in Figure 7 together with the results obtained from European observatories (Olsen, 1998); the lines represent the responses of D^+ models fitted to the different results. The expectation value of the misfit is $E\{\chi^2\} = 2 \cdot 7 = 14$ (real- and imaginary part of the observed response at seven periods). However, the actual χ^2 misfit of the models is much lower, as can be seen from Table III. This indicates that the estimated errors are probably too large. In order to be interpretable by 1-D models, $\text{Re}\{C\}$ has to increase with period T . This condition fails for the longest periods, which is probably due to the short time series. Therefore the responses at $T = 474$ h should be taken with care.

The apparent resistivities of the southern hemisphere are significantly higher than those of the northern hemisphere for all periods. This is an unexpected result, since the southern hemisphere is dominated by oceans, and analyses of ocean bottom data with the Z/H method (Bahr and Filloux, 1989) and magnetotellurics (Tarits et al., 1993a), respectively, indicate lower resistivity of the oceanic mantle.

TABLE III

C -responses, apparent resistivities ρ_a , phases ϕ and squared coherencies coh^2 for 7 periods T and different subdivisions of the Magsat evening data. L' is the effective number of data segments. Also listed is the χ^2 misfit of the D^+ models fitted to the various data sets

	T		Re $\{C\}$	Im $\{C\}$	δC	ρ_a	ϕ	coh^2	L'
	[s]	[h]	[km]	[km]	[km]	[Ωm]	[deg]		
Global ($\chi^2 = 2.8$)	151200	42	666	-180	73	24.9 ± 5.3	75 ± 16	0.954	73.1
	226800	63	831	-134	71	24.7 ± 4.2	81 ± 14	0.970	48.1
	340200	95	845	-210	72	17.6 ± 2.9	76 ± 13	0.979	31.9
	507600	141	841	-189	87	11.6 ± 2.3	77 ± 16	0.981	21.6
	761400	212	887	-240	86	8.8 ± 1.6	75 ± 14	0.988	15.2
	1139400	317	965	-277	166	7.0 ± 2.3	74 ± 25	0.974	9.0
	1706400	474	793	-142	271	3.0 ± 2.0	80 ± 54	0.967	6.3
Northern hemisphere ($\chi^2 = 0.4$)	151200	42	369	-293	128	11.6 ± 6.3	52 ± 28	0.861	72.0
	226800	63	438	-321	131	10.3 ± 5.0	54 ± 26	0.901	48.7
	340200	95	577	-267	118	9.4 ± 3.5	65 ± 24	0.945	32.6
	507600	141	598	-245	135	6.5 ± 2.7	68 ± 28	0.954	21.0
	761400	212	673	-267	145	5.4 ± 2.2	68 ± 27	0.966	14.1
	1139400	317	678	-236	279	3.6 ± 2.8	71 ± 55	0.926	9.2
	1706400	474	552	-238	327	1.7 ± 1.8	67 ± 73	0.950	6.2
Southern hemisphere ($\chi^2 = 7.0$)	151200	42	709	0	105	26.3 ± 7.8	90 ± 27	0.893	73.2
	226800	63	987	158	142	34.8 ± 9.9	99 ± 28	0.853	48.8
	340200	95	1005	-77	149	23.6 ± 7.0	86 ± 25	0.893	33.7
	507600	141	999	-157	164	15.9 ± 5.2	81 ± 26	0.917	20.6
	761400	212	1071	-170	165	12.2 ± 3.7	81 ± 25	0.944	13.5
	1139400	317	1099	-147	201	8.5 ± 3.1	82 ± 30	0.950	9.2
	1706400	474	973	42	394	4.4 ± 3.6	93 ± 75	0.905	6.5
Continents ($\chi^2 = 1.8$)	151200	42	439	-160	117	11.4 ± 5.7	70 ± 35	0.894	72.6
	226800	63	578	-269	112	14.1 ± 5.0	65 ± 23	0.933	48.9
	340200	95	668	-273	125	12.1 ± 4.2	68 ± 23	0.944	32.7
	507600	141	758	-249	124	9.90 ± 3.08	72 ± 22	0.962	21.5
	761400	212	679	-244	140	5.40 ± 2.09	70 ± 27	0.972	14.0
	1139400	317	752	-202	228	4.20 ± 2.46	75 ± 44	0.958	9.0
	1706400	474	557	-326	229	1.93 ± 1.37	60 ± 42	0.980	6.2
Oceans ($\chi^2 = 1.5$)	151200	42	678	-137	105	25.0 ± 7.6	79 ± 24	0.904	73.5
	226800	63	786	-158	92	22.4 ± 5.1	79 ± 18	0.950	48.2
	340200	95	879	-127	103	18.3 ± 4.3	82 ± 19	0.958	31.3
	507600	141	972	-193	100	15.3 ± 3.2	79 ± 16	0.972	21.5
	761400	212	956	-159	113	9.74 ± 2.27	81 ± 19	0.978	15.0
	1139400	317	965	-228	173	6.81 ± 2.38	77 ± 27	0.973	9.0
	1706400	474	900	-311	269	4.20 ± 2.37	71 ± 40	0.965	6.4

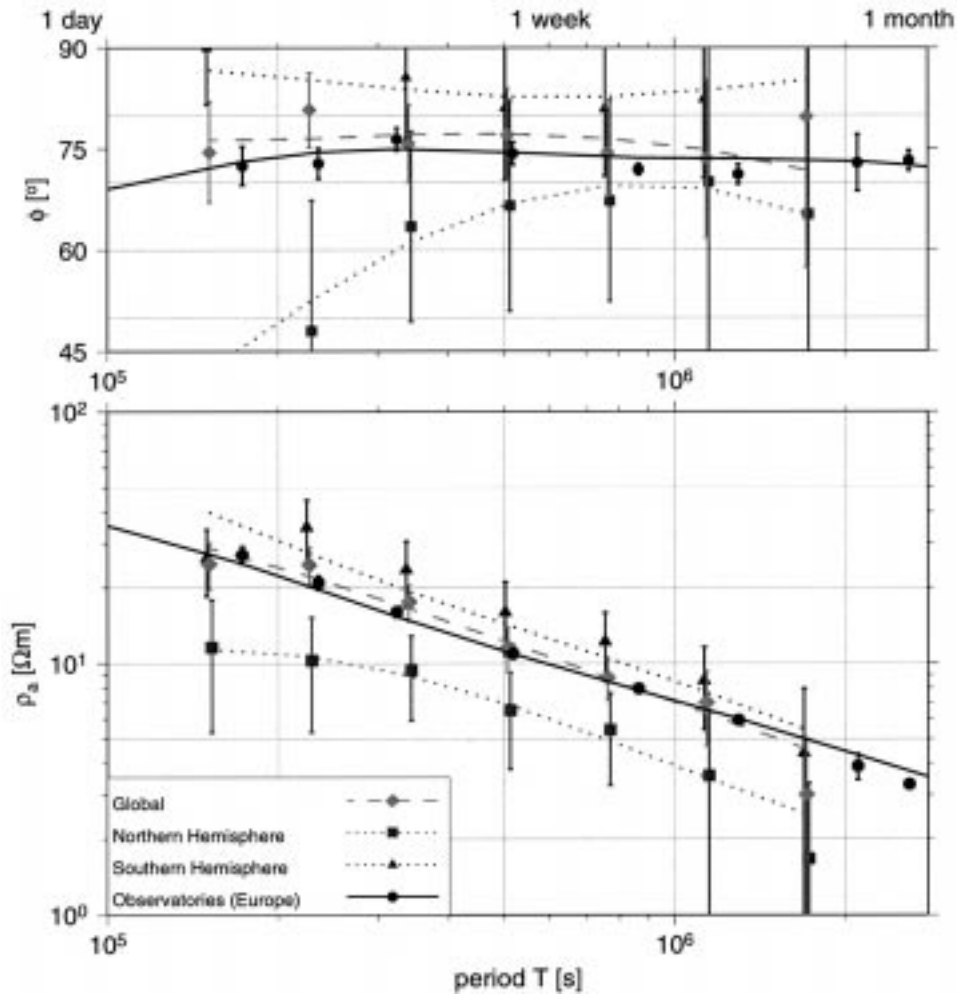


Figure 7. Apparent resistivities $\rho_a(a)$ and phases $\phi(a)$ obtained from the Magsat evening data and a subdivision of the measurements in northern and southern hemisphere data sets, respectively. Also shown are the results obtained from European observatories (Olsen, 1998). The lines represent the responses of D^+ models fitted to the different results.

To investigate this difference further, the data were re-analyzed but with a subdivision according to oceanic/continental regions. Figure 8 and the lower part of Table III presents the results of this analysis. It is observed that the oceanic apparent resistivities are higher than the continental for all periods, which is consistent with the result of the previous analysis (higher resistivity in the southern hemisphere). Surprisingly, however, the differences between the continental and oceanic regions are smaller than those between the northern and southern hemisphere. In addition, the difference does not disappear at longer periods, as one would expect if caused by the upper mantle conductivity. Model studies show that induction in the

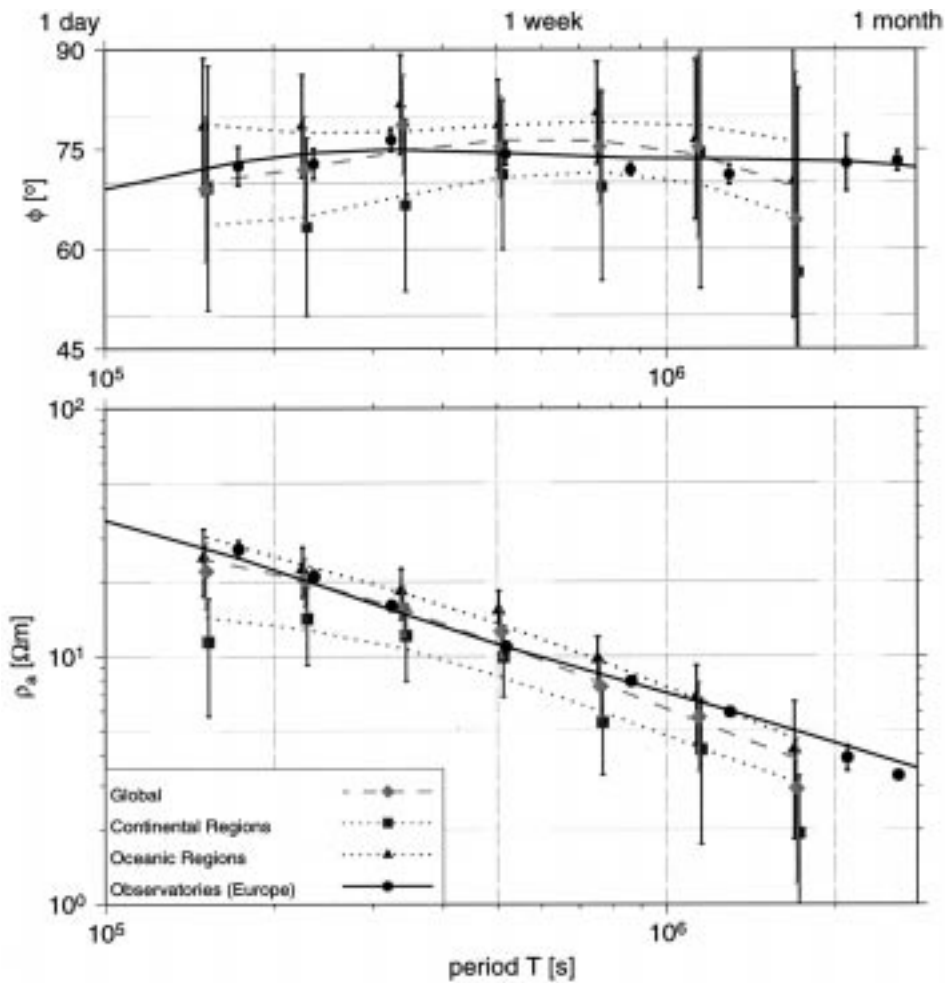


Figure 8. Same as Figure 7, but for a subdivision of the data according to oceanic and continental regions, respectively.

oceans is not able to explain this difference (see Section 5). Moreover, the northern hemisphere/continental resistivities are smaller than those found from European observatories (Olsen, 1998). All this indicates that the obtained values should be taken with care, and that probably other effects beside the different conductivity of the oceanic and continental mantle, respectively, contribute to the presented results.

The transfer functions could for instance be contaminated by ionospheric currents: the data were acquired during northern winter and hence the Sq current system was stronger in the southern hemisphere. However, it is rather unlikely that this would influence the responses almost equally at all periods up to 20 days. Another explanation could be the failure of the P_1^0 assumption, and hence other spherical harmonics have to be estimated, too. Their neglect could be respons-

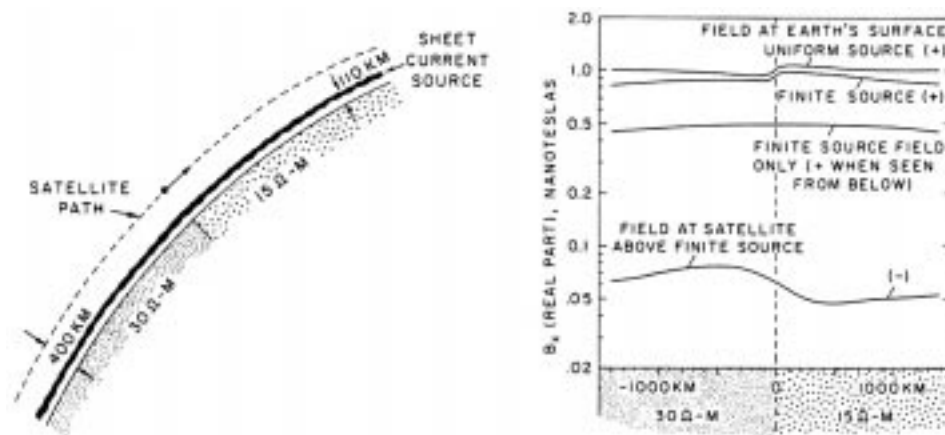


Figure 9. Left: Schematic of physical situation simulated by Hermance (1982). Right: The magnetic field component parallel to the direction of the satellite trajectory, for the period $T = 3$ h and an altitude of the satellite of 400 km. (After Hermance, 1982).

ible for the different responses in the northern and southern hemisphere. Future satellite missions will allow us to study this further.

4.5. INDUCTION STUDIES WITH SIGNALS FROM THE CORE

Magnetic field changes originating in the Earth's core can not reach the surface if their periods are much shorter than one year. This has been used for instance by MacDonald (1957) and Allredge (1977) to study lower mantle conductivity. Sudden geomagnetic core events (called "jerks") occur at the high-frequency end of the secular variation. They last only for about one year, or so, and are clearly observable at the Earth's surface and from satellites. Ground observations of jerks have been used by several authors to study the conductivity of the lower mantle and, especially, for determining an upper bound on deep mantle conductivity (Ducruix et al., 1980; Achache et al., 1981; Le Mouél and Courtillot, 1982). They used different assumptions about the time-space structure of the core field, and ended up with conductivities of the lower mantle between 1 and 1000 S/m. However, results from diamond-anvil laboratory measurements of lower mantle materials by (Shankland et al., 1993) suggest values between 1 and 10 S/m. The reason for this discrepancy is unknown, and further induction studies using jerks are needed to resolve it.

Though it is hard to observe jerks using satellites since they occur at random intervals, a jerk has been observed at many geomagnetic observatories in 1969–70, a period when magnetic measurements from the POGO satellites are also available. Backus et al. (1987) combined satellite and observatory data to test whether the observations of the jerk could be described by a model where the conductivity is almost spherically symmetric in the lower mantle and the time dependence of

the radial magnetic field component at the core-mantle boundary is either cubic, quintic, or biquadratic (two independent quadratics, one before and one after 1970). They found that the satellite data “do not require a jerk in 1969, but they permit it” and conclude: “At a high level of significance the parameters of the best fitting biquadratic rule out a physical model for the magnetic impulse of 1969 in which the level surfaces of electrical conductivity in the lower mantle are approximately spherical”.

Forthcoming satellites will measure the geomagnetic field for at least 5 years, which enhances the possibility to observe a geomagnetic jerk globally from space. This would certainly help to improve our understanding of deep mantle conductivity as well as core dynamics.

5. Model Studies

Hermance (1982) studied the effect of lateral conductivity heterogeneities on the magnetic field measured by a satellite at 400 km altitude crossing a major geological contact. The inducing source is assumed to be an ionospheric current system (with a horizontal wavelength of $2 \cdot 10^4$ km, corresponding to the large-scale source of Sq) so that both primary and secondary currents are below the satellite orbit. The ionospheric currents are associated with a magnetic field of 0.5 nT and vary with a period of 3 hours. The physical situation is sketched in the left part of Figure 9. The right part shows the results at ground (between the primary and the secondary currents) and at 400 km altitude. The resulting magnetic variation at satellite height is much smaller than it would be if the sources were above the satellite in the magnetosphere since both inducing and induced currents are internal and hence their magnetic field tend to cancel.

Tarits et al. (1993b) and Tarits (1994, 1997) studied the effect of mantle conductivity heterogeneities by solving the 3-D induction problem in a spherical Earth. They used a conductivity structure consisting of a layer at the Earth's surface describing the conductivity of the sea-water overlaying a 1-D model of mantle conductivity. However, large conductive bodies in the upper mantle due to subduction zones and continental roofs were also included. The magnetospheric ring current as well as the ionospheric Sq current system was used as external source models. From the results of this study the authors conclude that the induced part of the ionospheric Sq currents remains significant at satellite altitudes up to 800 km.

This results affects the accuracy of crustal field models and also the estimation of transfer functions. As mentioned in the introduction, regional induction studies using satellites are less influenced by local conductivity anomalies because of the height of the satellite. This holds of course also for induction in the oceans, and especially near coastlines (“coast effect”), as will be demonstrated by the following model study.

The external source is assumed to be of P_1^0 geometry (in geographic coordinates, however) with amplitude $\epsilon_1^0 = 10$ nT and a harmonic time dependency $e^{i\omega t}$ with $\omega = 2\pi/T$ and a period of $T = 2$ days. The conductivity of the mantle is given by the 4-layer 1-D model of Olsen (1998) overlaid by a thin shell representing the conductivity of the oceans. Its conductance is given by the oceanic bathymetry assuming 4 S/m for the conductivity of seawater. The “modified iterative-dissipative method” (Kuvshinov et al., 1999) is used to solve the induction equation on a 20×20 grid. Finally, the magnetic field components are determined at the Earth’s surface and at a satellite altitude of $h = 700$ km.

Figure 10 shows the real- and imaginary part of the magnetic radial component (external plus induced contributions) at ground (top panel) and at $h = 700$ km (lower panel). Without induction in the ocean, the magnetic field would be given by

$$B_r = \epsilon_1^0 \left[-1 + 2Q_1 \left(\frac{a}{r} \right)^3 \right] \cos \vartheta \quad (24)$$

with $\epsilon_1^0 = 10$ nT and $Q_1 = 0.348 + i0.041$ (this value follows from the model of mantle conductivity). From this equation it can be seen that the radial component is weaker at ground than at satellite altitude (due to $(a/r)^3$ and $2|Q_1| < 1$). This tendency holds when including the oceans, as seen in the Figure. However, induction in the ocean gives rise to other spherical harmonics than P_1^0 in the induced field, and using Equation (8) yields for the radial component

$$B_r = \epsilon_1^0 \left[-\cos \vartheta + 2 \sum_{n,m} q_{1n}^{0m} \left(\frac{a}{r} \right)^{n+2} P_n^m e^{im\lambda} \right]. \quad (25)$$

Consequently, small scale features (high spherical degree n) are more heavily damped at satellite altitudes due to $(a/r)^{n+2}$, which is also confirmed by the Figure.

This shows that the magnetic field at satellite altitude is less influenced by local conductivity anomalies compared to ground data, which is advantageous for studying large scale mantle heterogeneities and allows for a better determination of regional anomalies (for instance at continent/ocean transitions) with satellite data.

6. Conclusion

High-precision satellites in low altitude orbits provide considerable information about the Earth’s conductivity, in particular with respect to possible lateral heterogeneities of mantle conductivity. However, from the present analysis of the Magsat data it must be concluded that observatory data are probably more suitable than satellite data for studying the continental mantle conductivity due to the much longer time series. Forthcoming missions like Ørsted, SAC-C/Ørsted-2 and Champ

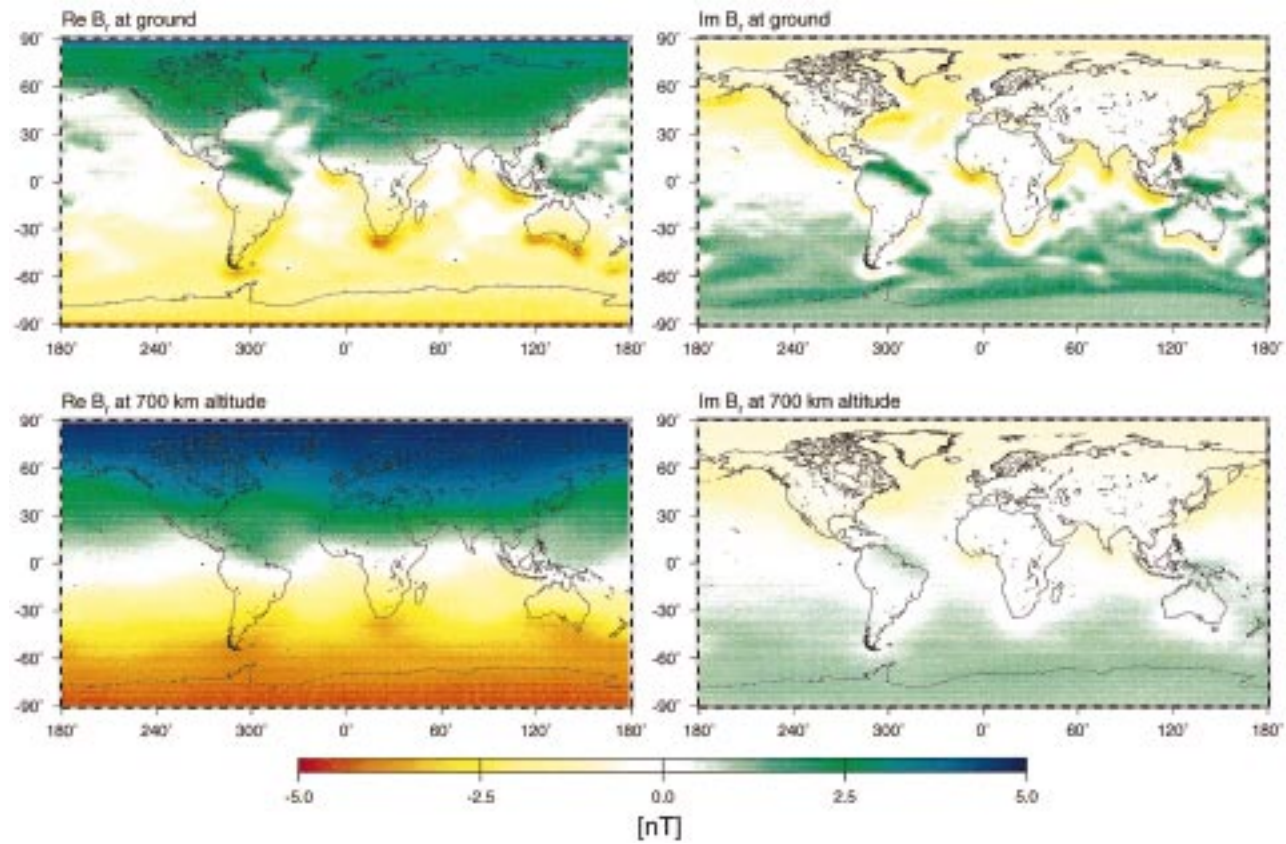


Figure 10. Real- and imaginary part of the magnetic radial component (external plus induced part) at the Earth's surface (top) and at 700 km altitude (bottom) for a P_1^0 -source of amplitude 10 nT and a harmonic time dependence with a period of $T = 2$ days.

though will extend the data base considerably, and it is expected that satellites may become an indispensable tool for investigating mantle conductivity.

However, proper consideration of the specialities of the satellite data must be made and methods developed for ground data should be applied only with care. This concerns for instance the question of the reference altitude of a response function.

In addition, new approaches for data analysis have to be developed. For instance: response functions at ground are usually estimated from times series which were measured at single points in space, whereas a satellite samples the magnetic field both in time and in space. Instead of binning the data and deriving responses for selected regions, it would be more convenient to have methods for the estimation of spatial functions of the responses.

To overcome the time-space ambiguity of the satellite observations, their combined analysis with ground data is promising. One could, for example, determine the space-time structure of magnetospheric current systems from a global net of ground observatories, which allows more spherical harmonic terms in addition to P_1^0 to be included. Comparison with the magnetic field observations by the satellite gives the possibility of estimating transfer functions without the restricting P_1^0 assumption.

The combined analysis of ground and satellite data also enables us to use ionospheric currents for induction studies. Langel et al. (1996) and Sabaka et al. (1999) describe "comprehensive models" of the near-Earth magnetic field. They used observatory and satellite data and solved simultaneously for sources in the core as well as in the ionosphere and magnetosphere; the most recent version of the model considers also contributions from the crust. Induction phenomena are treated in the present version of this model by means of an a priori 1-D conductivity model. Deviations from that 1-D model can be studied by subtracting model values from the satellite observations and analyzing the residuals. The subtracted model values, however, are synthesized using all but the induced part of the ionospheric contribution (and hence contain contributions from the core, the crust, the magnetosphere (plus its induced counterpart) and the ionosphere). Hence the time series of the residual field $\tilde{\mathbf{B}} = \tilde{\mathbf{B}}_{\text{obs}} - \tilde{\mathbf{B}}_{\text{mod}}$ consists only of the induced contribution due to ionospheric currents, plus noise. Comparison with the primary ionospheric field $\tilde{\mathbf{B}}_{\text{ion}}$ as predicted by the model then allows to study heterogeneities of mantle conductivity.

However, when using observatory data for induction studies on global scales one should keep in mind that the present distribution of ground observatories is far from ideal. Alexandrescu et al. (1994) and Langel et al. (1995) studied the impact of the distribution of the observatories on global field modeling, and Langel et al. (1995) discuss how this distribution can be improved: they propose 39 new observatories, 8 of which are ocean bottom magnetometers. Establishing ocean bottom magnetometers is a challenging task, but the authors demonstrate that even without

those the proposed distribution of observatories would decrease the estimated field model error by one order of magnitude.

Finally, it should be noted that multi-satellite missions are a very interesting and promising task. Regional induction studies will always suffer from the problem of aliasing if data from only one satellite are available. Future missions with more than one satellite in different orbits allow for monitoring the dynamic behavior of the Earth's magnetic field, which should be extremely helpful for induction studies from space.

Acknowledgements

I thank the committee of the working group I-2 of the IAGA for the invitation to give this tutorial at the 14th Workshop of Induction in the Earth in Sinaia, Romania in 1998. Furthermore, I am very grateful to Dana Abramova, Karsten Bahr, Bob Langel, Therese Moretto, Vladimir Semenov, Pascal Tarits and Ulrich Schmucker for suggestions and helpful discussions, and Alexei Kuvshinov for providing the code for the model studies presented in Section 5.

References

- Achache, I., Le Mouél, J.-L., and Courtillot, V.: 1981, 'Long-period geomagnetic variations and mantle conductivity: An inversion using Bailey's method', *Geophys. J. Roy. Astr. Soc.* **65**, 579–601.
- Alexandrescu, M., Duyen, C.H., and LeMouél, J.-L.: 1994, 'Geographical distribution of magnetic observatories and field modelling', *J. Geomagn. Geoelectr.* **46**, 891–901.
- Allredge, L.R.: 1977, 'Deep mantle conductivity', *J. Geophys. Res.* **82**(33), 5427–5431.
- Backus, G.E., Estes, R.H., Chino, D., and Langel, R.A.: 1987, 'Comparing the jerk with other global models of the geomagnetic field from 1960 to 1978', *J. Geophys. Res.* **92**, 3615–3622.
- Bahr, K. and Filloux, J.H.: 1989, 'Local S_q response function from EMSLAB data', *J. Geophys. Res.* **94**, 14,195–14,200.
- Banks, R.: 1969, 'Geomagnetic variations and the electrical conductivity of the upper mantle', *Geophys. J. Roy. Astr. Soc.* **17**, 457–487.
- Constable, S.: 1993, 'Constraints on mantle electrical-conductivity from field and laboratory measurements', *J. Geomagn. Geoelectr.* **45**(9), 7070–728.
- Didwall, E.M.: 1980, 'Continuous upper mantle conductivity models and their application to satellite data (abstract)', *EOS Trans. AGU* **61**, 226.
- Didwall, E.M.: 1981, 'The electrical conductivity of the Earth's upper mantle as estimated from satellite measured magnetic field variations', Ph.D. thesis, Johns Hopkins Univ., Baltimore, MD.
- Didwall, E.M.: 1984, 'The electrical conductivity of the upper mantle as estimated from satellite magnetic field data', *J. Geophys. Res.* **89**, 537–542.
- Didwall, E.M. and Langel, R.A.: 1976, 'Storm-time magnetic field variations: Implications for earth conductivity models (abstract)', *EOS Trans. AGU* **57**, 908.
- Didwall, E.M. and Langel, R.A.: 1977, 'Internal and external magnetic field variations as determined from satellite magnetic storm data (abstract)', *Trans. IAGA* **41**, 187.
- Dolginov, S.S.: 1972, 'Equatorial electrojet, according to KOSMOS-321 measurements', *Geomagn. Aeron.* **12**, 611–617.

- Ducruix, J., Courtillot, V., and Le Mouél, J.-L.: 1980, 'The late 1960s secular variation impulse, the eleven year magnetic variation and the electrical conductivity of the deep mantle', *Geophys. J. Roy. Astr. Soc.* **61**, 73–94.
- Hermance, J.F.: 1982, 'Model simulations of possible electromagnetic effects at MAGSAT activities', *Geophys. Res. Lett.* **9**, 373–376.
- Kendall, P.C. and Quinney, D.A.: 1983, 'Induction in the oceans', *Geophys. J. Roy. Astr. Soc.* **74**, 239–255.
- Kuvshinov, A.V., Avdeev, D.B., and Pankratov, O.V.: 1999, 'Global induction by *Sq* and *Dst* sources in the presence of oceans: Bimodal solutions for non-uniform spherical surface shells above radially symmetric Earth models in comparison to observations', *Geophys. J. Int.* **137**, 630–650.
- Langel, R.A.: 1975, 'Internal and external storm-time magnetic fields from spacecraft data (abstract)', *IGA Program Abstracts for XVI General Assembly*.
- Langel, R.A., Baldwin, R.T., and Green, A.W.: 1995, 'Toward an improved distribution of magnetic observatories for modeling of the main geomagnetic field and its temporal change', *J. Geomagn. Geoelectr.* **47**, 475–508.
- Langel, R.A. and Estes, R.H.: 1985, 'Large-scale, near-earth magnetic fields from external sources and the corresponding induced internal field', *J. Geophys. Res.* **90**, 2487–2494.
- Langel, R.A. and Hinze, W.J.: 1998, *The Magnetic Field of the Earth's Lithosphere: The Satellite Perspective*. Cambridge University Press.
- Langel, R.A., Sabaka, T.J., Baldwin, R.T., and Conrad, J.A.: 1996, 'The near-Earth magnetic field from magnetospheric and quiet-day ionospheric sources and how it is modeled', *Phys. Earth. Planet. Int.* **98**, 235–267.
- Le Mouél, J.-L. and Courtillot, V.: 1982, 'On the outer layers of the core and the geomagnetic secular variation', *J. Geophys. Res.* **87**, 4103–4108.
- MacDonald, K.L.: 1957, 'Penetration of the geomagnetic secular field through a mantle with variable conductivity', *J. Geophys. Res.* **62**, 117–141.
- Olsen, N.: 1998, 'Estimation of *C*-responses (3 h to 720 h) and the electrical conductivity of the mantle beneath Europe', *Geophys. J. Int.* **133**, 298–308.
- Oraevsky, V.N., Rotanova, N.M., Bondar, T.N., Abramova, D.Y., and Semenov, V.Y.: 1993a, 'On the radial geoelectrical structure of the mid-mantle from magnetovariational sounding using MAGSAT data', *J. Geomag. Geoelectr.* **45**, 1415–1423.
- Oraevsky, V.N., Rotanova, N.M., Dimitrev, V.I., Bondar, T.N., and Abramova, D.Y.: 1992a, 'Global magnetovariation sounding of the Earth according to MAGSAT satellite data', *Geomagn. Aeron.* **32**, 365–371.
- Oraevsky, V.N., Rotanova, N.M., Dimitrev, V.I., Bondar, T.N., and Abramova, D.Y.: 1992b, 'The result of deep magneto-variational probing of the Earth according to surface data and MAGSAT satellite measurements', *Geomagn. Aeron.* **33**, 235–239.
- Oraevsky, V.N., Rotanova, N.M., Semenov, V.Y., Bondar, T.N., and Abramova, D.Y.: 1993b, 'Magnetovariational sounding of the Earth using observatory and MAGSAT data', *Phys. Earth Planet Interior* **78**, 119–130.
- Parker, R.L.: 1980, 'The inverse problem of electromagnetic induction: Existence and construction of solutions based on incomplete data', *J. Geophys. Res.* **85**, 4421–4428.
- Parkinson, W.D. and Hutton, V.R.S.: 1989, 'The electrical conductivity of the Earth', in: J.A. Jacobs (ed.), *Geomagnetism*, Vol. 3. London: Academic Press, pp. 261–321.
- Roberts, R.G.: 1984, 'The long-period electromagnetic response of the Earth', *Geophys. J. Roy. Astr. Soc.* **78**, 547–572.
- Rotanova, N.M., Oraevsky, V.N., Semenov, V.Y., and Abramova, D.Y.: 1995, 'Regional magnetovariational sounding of the Earth with the use of MAGSAT data', *Geomagn. Aeron.* **34**, 531–536.
- Sabaka, T.J., Olsen, N., and Langel, R.A.: 1999, 'A comprehensive model of the near-Earth magnetic field: Phase 3', *Geophys. J. Int.*, in preparation.

- Schmucker, U.: 1970, 'Anomalies of geomagnetic variations in the Southwestern United States', *Bull. Scripps Inst. Ocean., University of California* **13**, 1–165.
- Schmucker, U.: 1985a, 'Electrical properties of the Earth's interior', in: *Landolt-Börnstein, New Series, 5/2b*. Springer-Verlag, Berlin-Heidelberg, pp. 370–397.
- Schmucker, U.: 1985b, 'Magnetic and electric fields due to electromagnetic induction by external sources', in: *Landolt-Börnstein, New Series, 5/2b*. Springer-Verlag, Berlin-Heidelberg, pp. 100–125.
- Schmucker, U.: 1987, 'Substitute conductors for electromagnetic response estimates', *PAGEOPH* **125**, 341–367.
- Schultz, A. and Larsen, J.C.: 1987, 'On the electrical conductivity of the mid-mantle – I. Calculation of equivalent scalar magnetotelluric response functions', *Geophys. J. Roy. Astr. Soc.* **88**, 733–761.
- Semenov, V., Ahramova, D., and Rotanova, N.: 1997, 'Regional geomagnetic soundings of the Earth's mantle using MAGSAT satellite measurements', *Acta geophysica polonica* **XLV**(1), 45–51.
- Shankland, T.J., Peyronneau, J., and Poirier, J.-P.: 1993, 'Electrical conductivity of the Earth's lower mantle', *Nature* **366**, 453–455.
- Takeda, M.: 1985, 'UT variation of internal S_q currents and the oceanic effect during 1980 March 1–18', *Geophys. J. Roy. Astron. Soc.* **80**, 649–659.
- Tarits, P.: 1994, 'Electromagnetic studies of global geodynamic processes', *Surveys in Geophysics* **15**, 209–238.
- Tarits, P.: 1997, 'Study of the 3-D mantle conductivity structure from Ørsted data (abstract no. 9)', in: E. Friis-Christensen and C. Skøtt (eds.), *Ørsted Compendium – Contributions from the International Science Team*. Copenhagen, Denmark.
- Tarits, P., Chave, A., and Schultz, A.: 1993a, 'Comment on "The Electrical Conductivity of the Oceanic Upper Mantle" by G. Heinson and S. Constable', *Geophys. J. Int.* **114**, 711–716.
- Tarits, P., Menvielle, M., and Wahr, J.: 1993b, 'Influence of crust and mantle heterogeneities on the internal response of the Earth by quiet field variations (abstract)', *IAGA 7th Scientific Assembly*, Buenos Aires.
- Van'yan, L.L., Faynberg, E.B., and Genis, N.Y.: 1975, 'Deep sounding of the Earth by ground-based and satellite measurements of the magnetic field of the equatorial electrojet', *Geomagn. Aeron.* **15**, 112–116.
- Winch, D.E.: 1989, 'Induction in a model ocean', *Phys. Earth Planet. Int.* **53**, 328–336.